MedChemComm

CONCISE ARTICLE

View Article Online
View Journal

Cite this: DOI: 10.1039/c4md00441h

Evaluation of aromatic 6-substituted thienopyrimidines as scaffolds against parasites that cause trypanosomiasis, leishmaniasis, and malaria†

Jennifer L. Woodring,[a] Gautam Patel,[a] Jessey Erath,[b] Ranjan Behera,[c] Patricia J. Lee,[d] Susan E. Leed,[d] Ana Rodriguez,[be] Richard J. Sciotti,[d] Kojo Mensa-Wilmot[c] and Michael P. Pollastri*[a]

Received 29th September 2014
Accepted 12th November 2014

DOI: 10.1039/c4md00441h

www.rsc.org/medchemcomm

Target repurposing is a proven method for finding new lead compounds that target *Trypanosoma brucei*, the causative agent of human African trypanosomiasis. Due to the recent discovery of a lapatinib-derived analog **2** with excellent potency against *T. brucei* (EC_{50} = 42 nM) and selectivity over human host cells, we have explored other classes of human tyrosine kinase inhibitor scaffolds in order to expand the range of chemotypes for pursuit. Following library expansion, we found compound **11e** to have an EC_{50} of 84 nM against *T. brucei* cells while maintaining selectivity over human hepatocytes. In addition, the library was tested against causative agents of Chagas' disease, leishmaniasis, and malaria. Two analogs with sub-micromolar potencies for *T. cruzi* (**4j**) and *Plasmodium falciparum* (**11j**) were discovered, along with an analog with considerable potency against *Leishmania major* amastigotes (**4e**). Besides identifying new and potent protozoan growth inhibitors, these data highlight the value of concurrent screening of a chemical library against different protozoan parasites.

Introduction

Human African trypanosomiasis (HAT) is a life-threatening parasitic disease that places 70 million people at risk in parts of sub-Saharan Africa. Caused by the protozoan parasite *Trypanosoma brucei*, it is one of 17 neglected tropical diseases (NTDs) highlighted by the World Health Organization as needing new therapies. Current medicines for HAT are not orally bioavailable, have unfavorable toxicity profiles and drug resistant parasites are emerging.[1]

Phosphodiesterase and kinase target repurposing[2] are rapid and pragmatic methods of lead drug discovery explored in our laboratory.[3–8] Launching new antiparasitic drug discovery efforts by redirecting inhibitors of human drug targets that are homologous to essential parasite targets or pathways can facilitate rapid development of structure–activity relationships (SAR), and accelerate "hit" optimization.

Inhibition of human receptor tyrosine kinases (RTKs) is a widely employed approach for cancer therapeutics.[9–12] Specifically, an epidermal growth factor receptor (EGFR) inhibitor lapatinib (GW572016, Tykerb, **1**, Fig. 1) was approved by the FDA in 2007 for solid tumors and breast cancer.[13–16] Compound **1** proved to be a promising lead for HAT due to its modest potency against *T. brucei* with an EC_{50} of 1.54 μM, and its ability to cure 25% of infected mice in a murine model of HAT.[17] Beginning with lapatinib, extensive SAR studies led to compound **2**, which has an EC_{50} of 42 nM and excellent selectivity over human cells. Importantly, compound **2** was orally bioavailable in mice and had a modest effect on parasitemia and life extension in a murine *T. brucei* bloodstream infection despite exhibiting high plasma protein binding (>99%) and a lack of central nervous system exposure.[7] These observed pharmacokinetic properties are not surprising due to its high log *P* and molecular weight.

The previous SAR explorations of the lapatinib chemotype focused on the "head" and "tail" regions of the molecule, described in Fig. 1. Historical tyrosine kinase inhibitor lead discovery efforts have led to many quinazoline scaffold replacements in cancer chemotherapy discovery.[18–21] GW837016X (**3**) possesses a related core scaffold and was also found to be potent

[a]*Northeastern University Department of Chemistry & Chemical Biology, 360 Huntington Avenue, Boston, MA 02115, USA. E-mail: m.pollastri@neu.edu; Tel: +1 617-373-2703*

[b]*New York University School of Medicine, Department of Microbiology, Division of Parasitology, 341 E. 25th St. New York, NY 10010, USA*

[c]*University of Georgia, Department of Cellular Biology, Athens, GA 30602, USA*

[d]*Experimental Therapeutics, Walter Reed Army Institute for Research, 2460 Linden Lane, Silver Spring, MD 20910, USA*

[e]*Anti-Infectives Screening Core, New York University School of Medicine, New York, NY 10010, USA*

† Electronic supplementary information (ESI) available: Synthetic preparations, assay details, *in vitro* ADME data, and additional malaria screening data are described in the ESI. See DOI: 10.1039/c4md00441h

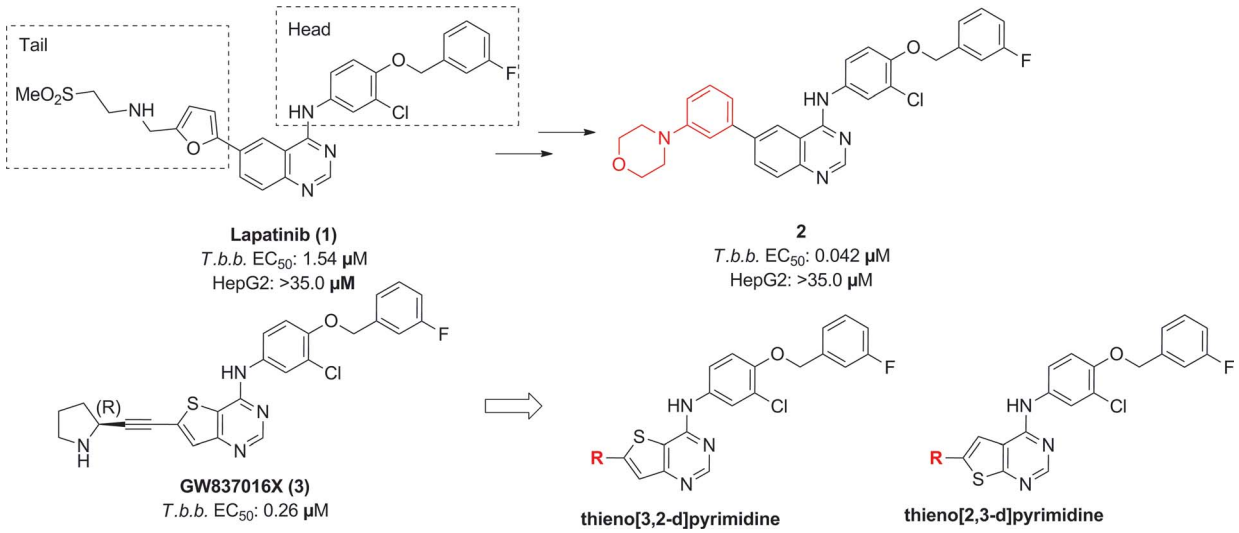

Fig. 1 Project strategy.

against *T. brucei*. It therefore seemed appropriate to utilize the thieno[3,2-*d*]pyrimidine (and the regioisomeric thieno[2,3-*d*]pyrimidine) scaffolds to launch a crossover SAR study, preparing analogs matched to those quinazoline-based inhibitors previously described[7] (denoted in this article as **4b–m**, Table 1).

We recently demonstrated the value of simultaneously testing compounds against related protozoan parasites, wherein it became evident that producing parasite-dependent SAR could direct future work against each pathogen.[8] In addition to the screening of new compounds against *T. brucei*, compounds were screened against the kinetoplastid parasites *Leishmania major* (causative agent of cutaneous leishmaniasis) and *T. cruzi* (which causes Chagas disease), as well as the malaria-causing parasite *Plasmodium falciparum*. In this report we disclose the results of our efforts to prepare and test thienopyrimidine-based inhibitors, matching the "tail" replacements explored in the previous study that led to compound **2**.[7]

Synthetic procedure

The requisite dihalo template precursors (**9** and **16**, Schemes 1 and 2) of the thieno[3,2-*d*]pyrimidine and thieno[2,3-*d*]pyrimidine scaffolds were made following previously disclosed protocols.[22–25] The thieno[3,2-*d*]pyrimidine intermediate **9** was synthesized starting from methyl 3-aminothiophene-2-carboxylate (**5**) as shown in Scheme 1. This commercially available material underwent formylation, followed by cyclization with formamide and ammonium formate to afford intermediate **7**. The pyrimidinone **7** was chlorinated using phosphorous oxychloride to provide **8** and brominated using 1,2-dibromo-1,1,2,2-tetrafluoroethane to yield the key thienopyrimidine **9**. From this point, halide displacement with the requisite aniline in refluxing isopropanol produced the bromide intermediate **10**, amenable for subsequent Suzuki chemistry.

The thieno[2,3-*d*]pyrimidine template was synthesized from commercially available methyl 2-cyanoacetate (**12**, Scheme 2), which underwent Gewald reaction conditions with 1,4-dithiane-2,5-diol to produce the desired aminothiophene **13**. Cyclization of the thiophene with formamide afforded intermediate **14**, followed by sequential bromination (**15**), and chlorination to provide **16**. As before, aniline displacement of the chloride was effected smoothly, providing **17** for further diversification *via* Suzuki reaction. For both scaffolds, intermediate **10** or intermediate **17** was coupled with boronic esters or acids using Suzuki reaction conditions to generate the respective final compounds **11a–m** and **18a–j**, which are matched with corresponding quinazoline analogs previously reported (Table 1).[7]

Results and discussion

Tests of the compounds against *T. brucei* revealed favorable growth inhibitory activity amongst three distinct scaffolds shown in Table 1. To make the direct comparison with **2**, replacement of the quinazoline with thieno[2,3-*d*]pyrimidine (**18a**) yielded a 10× change in potency, whereas the thieno[3,2-*d*]pyrimidine replacement (**11a**) resulted in a dramatic loss of potency. Removal of the morpholine altogether (**4b**, **11b**, **18b**) or the tail altogether (**4m**, **11m**) reduced the potency to the micromolar range.

An additional atom linker between the phenyl and morpholine was more favored on the quinazoline scaffold (**4j**) than the thienopyrimidines (**11j** and **18j**) but still showed reduced potency. Evaluation of the morpholine regiochemistry revealed that *para* (**4k**, **11k**) was less potent than *meta* (**2**, **11a**, **18a**), though alteration of this regiochemistry was better tolerated when attached to the thieno[3,2-*d*]pyrimidine (**11k**) than the quinazoline scaffold (**4k**). The most potent compound from this series is **11e**, an 84 nM inhibitor of *T. brucei* cell growth. This "tail" was not as potent in the quinazoline scaffold (**4e**); the morpholinophenyl tail present in **2** remains the most potent analog overall with an EC_{50} of 42 nM. For the most potent analogs in the thieno[2,3-*d*]pyrimidine scaffold, both the 5-methyl-6-morpholinopyridin-3-yl tail (**18e**) and the morpholinophenyl tail (**18a**) were essentially equipotent with EC_{50} values

Table 1 Antiparasitic activities of compounds against *T. brucei*, *T. cruzi*, *L. major*, and *P. falciparum*

Cmpd	Scaffold[a]	R	*T. brucei* EC_{50} (μM) or % inh (at 5 μM)[b]	*T. cruzi* EC_{50} (μM) or % inh (at 10 μM)[b]	*L. major* Amast EC_{50} (μM)[c]	*L. major* Promast EC_{50} (μM)[c]	*P. falciparum* D6 EC_{50} (μM)[d]
2[e]	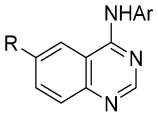	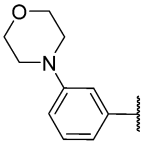	0.042 ± 0.010	1.8 ± 0.9	7.98 $r^2 = 0.75$	2.97 $r^2 = 0.76$	0.23 $r^2 = 0.99$
11a	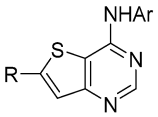		42%	>50	5.4 $r^2 = 0.81$	>20	0.86 $r^2 = 0.98$
18a	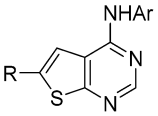		0.40 ± 0.05	2.2 ± 0.4	2.60 $r^2 = 0.94$	>20	0.52 $r^2 = 0.99$
4b[e]	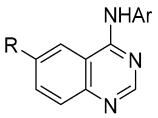		3.9 ± 0.3	1.8 ± 0.1	>15	4.05 $r^2 = 0.85$	0.79 $r^2 = 0.90$
11b	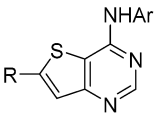	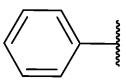	2.8 ± 0.1	0%	>15	8.14 $r^2 = 0.86$	2.97 $r^2 = 0.98$
18b[f]	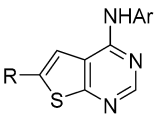		1.7 ± 0.2	42%	>15	>20	>20
4c[e]	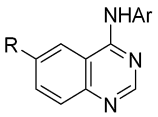	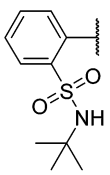	4.7 ± 0.2	6.4 ± 4.0	Nd[g]	Nd[g]	*n*[g]
11c	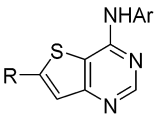		1.2 ± 0.1	0.67 ± 0.06	2.37 $r^2 = 0.92$	>20	1.07 $r^2 = 0.96$
18c	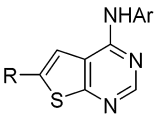		0.5 ± 0.2	>50.0	>15	>20	>15
4d[e]	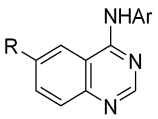	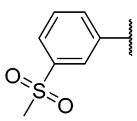	3.2 ± 0.1	5.0 ± 0.0	4.67 $r^2 = 0.91$	3.49 $r^2 = 0.82$	0.52 $r^2 = 0.98$
11d	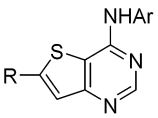		1.4 ± 0.0	2.7 ± 2.3	>3	>3	0.65 $r^2 = 0.96$
18d	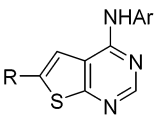		1.3 ± 0.1	2.4 ± 1.0	>15	11.75 $r^2 = 0.90$	0.52 $r^2 = 0.97$

Table 1 (*Contd.*)

Cmpd	Scaffold[a]	R	*T. brucei* EC_{50} (μM) or % inh (at 5 μM)[b]	*T. cruzi* EC_{50} (μM) or % inh (at 10 μM)[b]	*L. major* Amast EC_{50} (μM)[c]	*L. major* Promast EC_{50} (μM)[c]	*P. falciparum* D6 EC_{50} (μM)[d]
4e	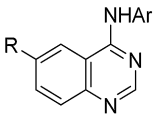		1.0 ± 0.1	49%	1.14 $r^2 = 0.85$	>20	0.26 $r^2 = 0.96$
11e	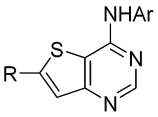	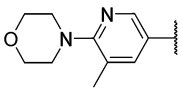	0.084 ± 0.0	3.3 ± 1.2	>3	>3	0.23 $r^2 = 0.98$
18e	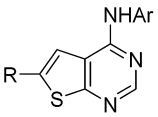		0.42 ± 0.1	29%	>3	>3	0.28 $r^2 = 0.99$
4f	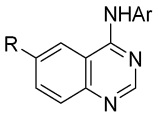		0.22 ± 0.00	2.2 ± 0.4	4.09 $r^2 = 0.92$	>20	0.60 $r^2 = 0.96$
11f	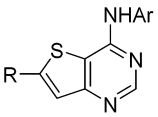	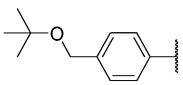	0.89 ± 0.10	30 ± 13	>15	>20	1.65 $r^2 = 0.98$
18f	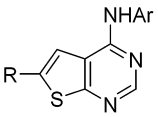		1.6 ± 0.0	17%	2.03 $r^2 = 0.84$	>20	7.79 $r^2 = 0.93$
4g[e]	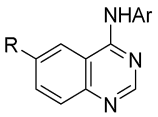		5.3 ± 0.2	Nd	>15	6.86 $r^2 = 0.78$	5.79 $r^2 = 0.98$
11g	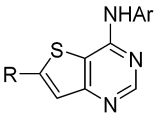	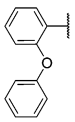	10%	>50.0	3.50 $r^2 = 0.84$	>20	6.21 $r^2 = 0.46$
18g	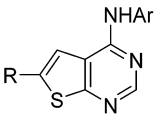		1.2 ± 0.3	45%	>15	>20	10.78 $r^2 = 0.94$
4h[e]	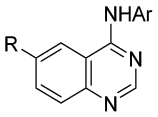		0.14 ± 0.1	>50.0	>15	>3	0.51 $r^2 = 0.98$
11h	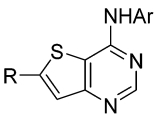	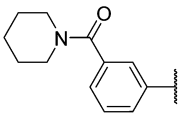	46%	3.2 ± 0.5	3.10 $r^2 = 0.93$	>20	1.17 r^2 =0.94
18h	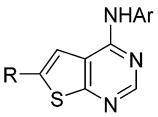		0.33 ± 0.03	>50.0	>15	>20	2.11 $r^2 = 0.98$

Table 1 (*Contd.*)

Cmpd	Scaffold[a]	R	*T. brucei* EC_{50} (μM) or % inh (at 5 μM)[b]	*T. cruzi* EC_{50} (μM) or % inh (at 10 μM)[b]	*L. major* Amast EC_{50} (μM)[c]	*L. major* Promast EC_{50} (μM)[c]	*P. falciparum* D6 EC_{50} (μM)[d]
4i[e]	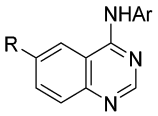		6.0 ± 0.2	>50.0	>15	>20	0.91 $r^2 = 0.99$
11i	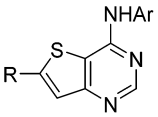	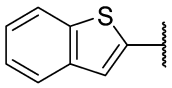	8%	>50.0	>15	>20	>15
18i	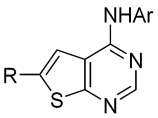		2.9 ± 0.3	49%	>3	>3	>4
4j[e,f]	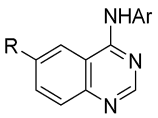		1.0 ± 0.05	0.60 ± 0.15	5.91 $r^2 = 0.94$	2.74 $r^2 = 0.88$	0.063 r^2 =0.99
11j	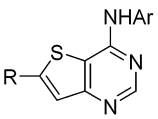	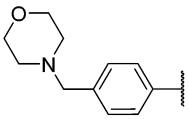	1.1 ± 0.0	>50.0	>15.0	0.22 $r^2 = 0.84$	0.027 $r^2 = 0.97$
18j	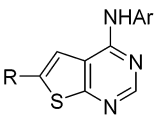		60%	1.7 ± 0.1	4.20 $r^2 = 0.91$	>20	0.089 $r^2 = 0.81$
4k[e,f]	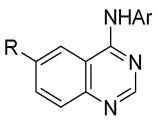	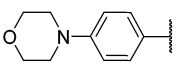	1.9 ± 0.9	10.1%	>15	4.40 $r^2 = 0.82$	0.27 $r^2 = 0.98$
11k	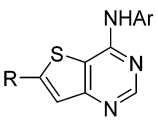		0.47 ± 0.25	0%	>15	>20	3.10 $r^2 = 0.98$
4l[e]	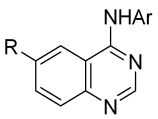	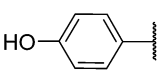	6.5 ± 1.0	>50.0	>15	>20	>20
11l	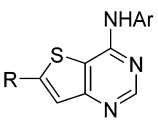		2.2 ± 0.1	0.75 ± 0.02	1.58 $r^2 = 0.83$	>20	0.44 $r^2 = 0.98$

Table 1 (*Contd.*)

Cmpd	Scaffold[a]	R	*T. brucei* EC_{50} (μM) or % inh (at 5 μM)[b]	*T. cruzi* EC_{50} (μM) or % inh (at 10 μM)[b]	*L. major* Amast EC_{50} (μM)[c]	*L. major* Promast EC_{50} (μM)[c]	*P. falciparum* D6 EC_{50} (μM)[d]
4m	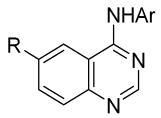	H	1.3 ± 0.1	2.4 ± 0.2	12.36 $r^2 = 0.78$	1.75 $r^2 = 0.77$	5.33 $r^2 = 0.69$
11m	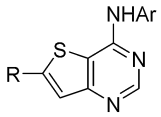		1%	27 ± 3.5	>15	5.68 $r^2 = 0.94$	16.4 $r^2 = 0.93$

[a] Ar is defined as 3-chloro-4-((3-fluorobenzyl)oxy)phenyl. [b] Compounds showing >75% growth inhibition at 5 or 10 μM for *T. brucei* or *T. cruzi*, respectively, were tested for EC_{50} values. *T. brucei* EC_{50} values are the result of duplicate experiments, within ±25%, with the exception of **11e** (±33%), and **11k** (±52%). *T. cruzi* EC_{50} values are the result of duplicate experiments, within ±50%, with the exception of **4c** (±63%), and **11d** (±85%). [c] Compounds screened against *L. major* amastigotes and promastigotes were tested in duplicate and had r^2 values >0.75. [d] Compounds were tested in duplicate against *P. falciparum* (D6 strain) and had r^2 values >0.90 except for **11g** ($r^2 = 0.46$) and **18j** ($r^2 = 0.81$) against *P. falciparum*. [e] Previously reported data utilizing the same assay as described in the ESI.[7] [f] All compounds were inactive against HepG2 cell lines except for **4b** ($TC_{50} = 4.9$ μM), **4j** (12.9 μM), **4k** (9.6 μM), and **18b** (10.0 μM). [g] Not determined due to low solubility in the assay conditions.

of 420 and 400 nM respectively, but the 3-phenyl(piperidin-1-yl) methanone analog (**18h**) was slightly more potent with an EC_{50} of 330 nM.

Fig. 2 displays the effect of changing the scaffold, while maintaining the R-group substitution, upon anti-*T. brucei* activity. We can make a few observations from this qualitative analysis. First, in the majority of cases, switching from

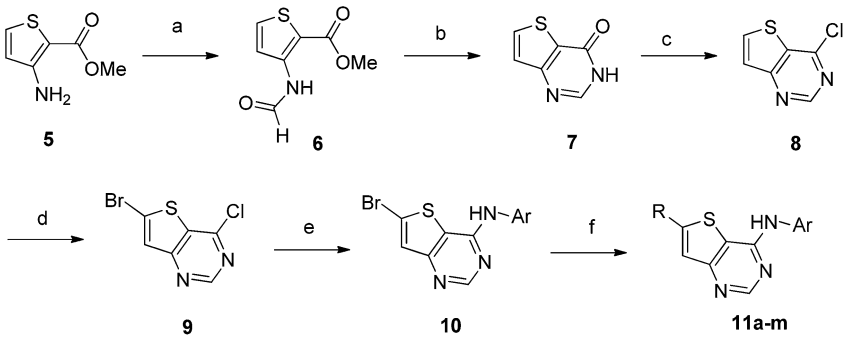

Scheme 1 Synthesis of the thieno[3,2-*d*]pyrimidine template. Reagents and conditions: (a) HCO_2H, Ac_2O, 0 °C to RT, 12 h, 79%; (b) $HCONH_2$, NH_4HCO_2, 150 °C to RT, 17 h, 56%; (c) $POCl_3$, 110 °C, 12 h, 90%; (d) LDA, $C_2Br_2F_4$, THF, −78 °C to RT, 13 h, 94%; (e) 3-chloro-4-((3-fluorobenzyl) oxy)aniline, IPA, 85 °C, 12 h, 88%; (f) boronic ester, Na_2CO_3, $Pd(PPh_3)_4$, DME/EtOH (3 : 2), H_2O, 80–85 °C, 12 h, 8–36%.

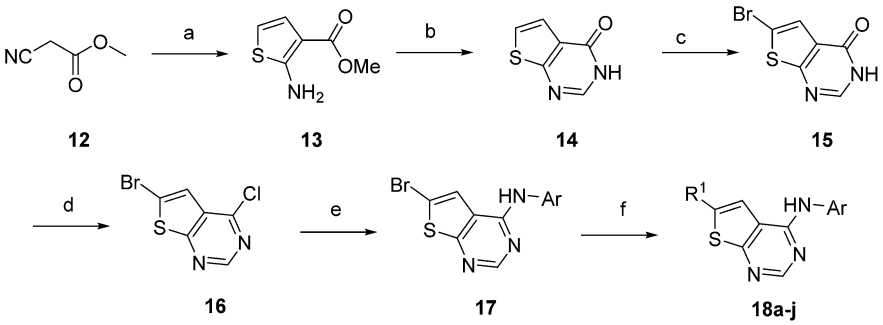

Scheme 2 Synthesis of the thieno[2,3-*d*]pyrimidine template. Reagents and conditions: (a) 1,4-dithiane-2,5-diol, TEA, DMF, 45 °C, 2 h, 58%; (b) $HCONH_2$, 170 °C, 6 h, 38%; (c) Br_2, AcOH, 80 °C, 2 h, 79%; (d) $POCl_3$, 100 °C, 12 h, 75%; (e) 3-chloro-4-((3-fluorobenzyl)oxy)aniline, IPA, 85 °C, 12 h, 88%; (f) boronic ester, Na_2CO_3, $Pd(PPh_3)_4$, DME/EtOH (3 : 2), H_2O, 85 °C, 12 h, 20–46%.

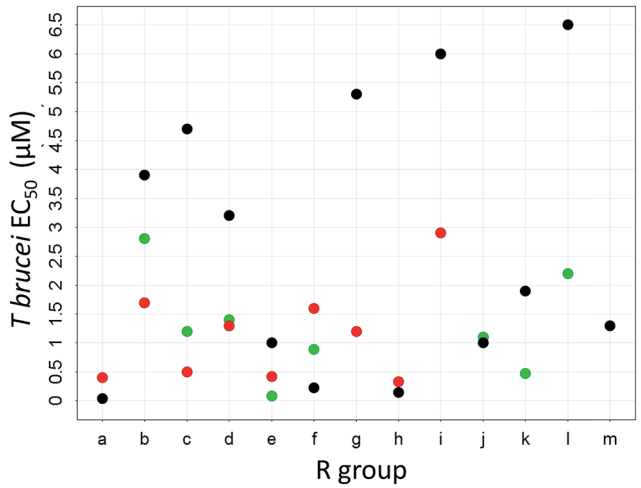

Fig. 2 Plot of anti-trypanosome activity as a function of R-group (*X*-axis) and scaffold (black = quinazoline, red = thieno[2,3-*d*]pyrimidine; green = thieno[3,2-*d*]pyrimidine). R group letter corresponds to compound substitutions listed in Table 1.

quinazoline (black circles) to thieno[2,3-*d*]pyrimidine (red circles) tends to improve compound potency (*i.e.*, reduces EC_{50} 3-fold or more). Second, when comparing matched analogs between the quinazoline and thieno[3,2-*d*]pyrimidine scaffolds, except for **18c** *versus* **4c**, which is about a 9-fold difference; 0.5 *versus* 4.7 μM, the difference in activity is seldom greater than two-fold. This indicates that thieno[3,2-*d*]pyrimidines, unlike thieno[2,3-*d*]pyrimidines, are equipotent to quinazolines when tested against *T. brucei*. Third, the range of activities for compounds with thienopyrimidine scaffolds is narrower (0.084–2.9 μM) than the quinazolines (0.042–6.5 μM). Fourth, for matched pairs of the [3,2-*d*] and [2,3-*d*] scaffold, there is seldom more than a 2-fold difference in EC_{50} (the only exception being **11j** (EC_{50} = 1.1 μM) *vs.* **18j**, which only inhibits parasite growth 60% at 5 μM).

Table 1 also shows the results of testing these analogs against the other protozoan parasites. Compound **2** and its related thienopyrimidine-derived analogs **11a** and **18a** had shown sub-micromolar potency towards the malaria parasite *P. falciparum*. Removal of the "tail" (**4m**, **11m**) or of the morpholine (**4b**, **11b**, **18b**) produced a significant loss in potency across all 3 scaffolds. *Ortho* substitution on the phenyl portion of the tail was not well tolerated by any set tested. The three tails that produced the most potent analogs were the *meta* substituted methylsulfonyl (**4d**, **11d**, **18d**), the *para* substituted methyl-pyridinylmorpholine (**4e**, **11e**, **18e**), and the *para* substituted benzylmorpholine (**4j**, **11j**, **18j**). These tails consistently showed sub-micromolar EC_{50} values across all three scaffolds, suggesting that appropriately placed H-bond acceptors may be crucial to antimalarial activity in this region. These compounds were also tested against two drug resistant strains of malaria (W2, C235) and were generally found to show potencies within 3-fold of the D6 strain (Table S2, Fig. S1 (ESI†)).

Although **2** and the corresponding thieno[2,3-*d*]pyrimidine analog **18a** displayed promising micromolar potency against *T. cruzi*, overall the thieno[3,2-*d*]pyrimidine analogs were more potent in this study, with the best compounds being **4j** (EC_{50} = 0.60 μM), **11c** (0.67 μM), and **11l** (0.75 μM). Quinazolines tolerated the removal of the morpholino group better than either of the thienopyrimidines. Though the *para*-morpholinophenyl tail (**4k**, **11k**) was inactive in this assay, adding an intervening methylene group (**4j** and **11l**) resulted in active analogs.

Screening of more than 35 compounds against amastigotes of *Leishmania major* failed to produce any sub-micromolar compounds. The most potent analog across all 3 scaffolds against *Leishmania major* amastigotes was **4e** with an EC_{50} of 1.14 μM. Against promastigotes of *L. major* only **11j** had sub-micromolar potency (EC_{50} = 220 nM). As seen with other drug sensitivity studies, there is often little-to-no correlation between the effect of compounds on intracellular amastigotes and the promastigote form of *Leishmania*.[26]

Most compounds showed no toxicity to the HepG2 cell line except **4b**, **4j**, **4k**, and **18b** with TC_{50} values (concentration leading to 50% growth inhibition of host cells) of 4.9, 12.9, 9.6, and 10.0 μM respectively.

We tested the two most potent *T. brucei* growth inhibitors **2** and **11e** in *in vitro* ADME assays, and observed that, as predicted based on their high *c* log *P* (7.6 and 7.4 respectively), both have poor solubility (<1 μM), high protein binding (>99%), and modest metabolic stability (Table S3, ESI†). Nonetheless, as the goal of this report was to describe SAR between the quinazoline and thienopyrimidine scaffolds, we are encouraged by the reasonable SAR tracking that is observed between the different scaffolds. Work continues on all three scaffolds to improve their physicochemical properties, primarily focused upon reducing size and lipophilicity; results will be reported in due course.

Conclusions

We have previously shown that some lapatinib-derived analogs have high potency towards the HAT parasite *T. brucei* and with little host cell toxicity, typified by **2** (EC_{50} = 42 nM). In assessing matched [3,2-*d*] and [2,3-*d*] thienopyrimidine scaffold replacements, we have discovered analogs, such as **11e**, that have excellent potency against *T. brucei* cells (EC_{50} = 84 nM). Also, a multi-pathogen testing campaign using these *T. brucei* inhibitors against select protozoan parasites produced compounds with a variety of favorable potencies: **4j**, *T. cruzi* EC_{50} = 0.60 μM; **4e**, *L. major* amastigote EC_{50} = 1.14 μM and **11j**, *P. falciparum* EC_{50} = 0.027 μM. While these data are indicative of good starting points for antiparasite drug discovery, attention must be paid to improvement of the physicochemical properties of these agents in order to produce effective drugs.

Acknowledgements

This work was funded in part by NIH grants R01AI082577 (MPP), R56AI099476 (MPP and KM-W), and R21AI076647 (KM-W). We thank GlaxoSmithKline for providing GW837016X that was used in exploratory studies with *T. brucei*. We appreciate a free academic license for the OpenEye suite of software, and are

grateful to AstraZeneca for performing the *in vitro* ADME experiments described in this manuscript.

References

1 World Health Organization Fact Sheet No. 259, http://www.who.int/mediacentre/factsheets/fs259/en/, accessed 28 July 2014.
2 M. P. Pollastri and R. K. Campbell, *Future Med. Chem.*, 2011, **3**, 1307–1315.
3 N. D. Bland, C. Wang, C. Tallman, A. E. Gustafson, Z. Wang, T. D. Ashton, S. O. Ochiana, G. McAllister, K. Cotter, A. P. Fang, L. Gechijian, N. Garceau, R. Gangurde, R. Ortenberg, M. J. Ondrechen, R. K. Campbell and M. P. Pollastri, *J. Med. Chem.*, 2011, **54**, 8188–8194.
4 R. Diaz-Gonzalez, F. M. Kuhlmann, C. Galan-Rodriguez, L. M. d. Silva, M. Saldivia, C. E. Karver, S. M. Beverley, A. Rodriguez, M. Navarro and M. P. Pollastri, *PLoS Neglected Trop. Dis.*, 2011, **5**, e1297.
5 J. D. Seixas, S. A. Luengo-Arratta, R. Diaz, M. Saldivia, D. I. Rojas-Barros, P. Manzano, S. Gonzalez, M. Berlanga, T. K. Smith, M. Navarro and M. P. Pollastri, *J. Med. Chem.*, 2014, **57**, 4834–4848.
6 S. O. Ochiana, V. Pandarinath, Z. Wang, R. Kapoor, M. J. Ondrechen, L. Ruben and M. P. Pollastri, *Eur. J. Med. Chem.*, 2013, **62**, 777–784.
7 G. Patel, C. E. Karver, R. Behera, P. J. Guyett, C. Sullenberger, P. Edwards, N. E. Roncal, K. Mensa-Wilmot and M. P. Pollastri, *J. Med. Chem.*, 2013, **56**, 3820–3832.
8 G. Patel, N. E. Roncal, P. J. Lee, S. E. Leed, J. Erath, A. Rodriguez, R. J. Sciotti and M. P. Pollastri, *MedChemComm*, 2014, **5**, 655–658.
9 G. S. Cockerill and K. E. Lackey, *Curr. Top. Med. Chem.*, 2002, **2**, 1001–1010.
10 P. Traxler, *Expert Opin. Ther. Targets*, 2003, **7**, 215–234.
11 J. Baselga and C. L. Arteaga, *J. Clin. Oncol.*, 2005, **23**, 2445–2459.
12 N. E. Hynes and H. A. Lane, *Nat. Rev. Cancer*, 2005, **5**, 341–354.
13 D. W. Rusnak, K. Lackey, K. Affleck, E. R. Wood, K. J. Alligood, N. Rhodes, B. R. Keith, D. M. Murray, W. B. Knight, R. J. Mullin and T. M. Gilmer, *Mol. Cancer Ther.*, 2001, **1**, 85–94.
14 W. Xia, R. J. Mullin, B. R. Keith, L. H. Liu, H. Ma, D. W. Rusnak, G. Owens, K. J. Alligood and N. L. Spector, *Oncogene*, 2002, **21**, 6255–6263.
15 S. R. Johnston and A. Leary, *Drugs Today*, 2006, **42**, 441–453.
16 B. Moy, P. Kirkpatrick, S. Kar and P. Goss, *Nat. Rev. Drug Discovery*, 2007, **6**, 431–432.
17 R. Behera, S. M. Thomas and K. Mensa-Wilmot, *Antimicrob. Agents Chemother.*, 2014, **58**, 2202–2210.
18 A. G. Waterson, K. G. Petrov, K. R. Hornberger, R. D. Hubbard, D. M. Sammond, S. C. Smith, H. D. Dickson, T. R. Caferro, K. W. Hinkle, K. L. Stevens, S. H. Dickerson, D. W. Rusnak, G. M. Spehar, E. R. Wood, R. J. Griffin and D. E. Uehling, *Bioorg. Med. Chem. Lett.*, 2009, **19**, 1332–1336.
19 K. L. Stevens, K. J. Alligood, J. G. Alberti, T. R. Caferro, S. D. Chamberlain, S. H. Dickerson, H. D. Dickson, H. K. Emerson, R. J. Griffin, R. D. Hubbard, B. R. Keith, R. J. Mullin, K. G. Petrov, R. M. Gerding, M. J. Reno, T. R. Rheault, D. W. Rusnak, D. M. Sammond, S. C. Smith, D. E. Uehling, A. G. Waterson and E. R. Wood, *Bioorg. Med. Chem. Lett.*, 2009, **19**, 21–26.
20 R. D. Hubbard, S. H. Dickerson, H. K. Emerson, R. J. Griffin, M. J. Reno, K. R. Hornberger, D. W. Rusnak, E. R. Wood, D. E. Uehling and A. G. Waterson, *Bioorg. Med. Chem. Lett.*, 2008, **18**, 5738–5740.
21 E. R. Wood, L. M. Shewchuk, B. Ellis, P. Brignola, R. L. Brashear, T. R. Caferro, S. H. Dickerson, H. D. Dickson, K. H. Donaldson, M. Gaul, R. J. Griffin, A. M. Hassell, B. Keith, R. Mullin, K. G. Petrov, M. J. Reno, D. W. Rusnak, S. M. Tadepalli, J. C. Ulrich, C. D. Wagner, D. E. Vanderwall, A. G. Waterson, J. D. Williams, W. L. White and D. E. Uehling, *Proc. Natl. Acad. Sci. U. S. A.*, 2008, **105**, 2773–2778.
22 T. R. Caferro, S. D. Chamberlain, K. H. Donaldson, P. A. Harris, M. D. Gaul, D. E. Uehling and D. E. Vanderwall, WO2003053446A1, 2003.
23 M. A. Benish, R. J. A. Budde and M. Lawless, WO2002057271A2, 2002.
24 B. Buchmann, N. Braeuer, M. Koppitz, O. Peters, L. A. Ter, B. Lindenthal, G. Langer and T. Wintermantel, WO2009007421A1, 2009.
25 Y. Huang, S. Wolf, M. Bista, L. Meireles, C. Camacho, T. A. Holak and A. Dömling, *Chem. Biol. Drug Des.*, 2010, **76**, 116–129.
26 G. De Muylder, K. K. Ang, S. Chen, M. R. Arkin, J. C. Engel and J. H. McKerrow, *PLoS Neglected Trop. Dis.*, 2011, **5**, e1253.

